Acta Neuropathol (2005) 109: 339–345
DOI 10.1007/s00401-004-0955-7

CASE REPORT

**Akiyoshi Kakita · Chikanori Inenaga
Shigeki Kameyama · Hiroshi Masuda · Takehiko Ueno
Junpei Honma · Mitsuteru Shimohata
Hitoshi Takahashi**

Cerebral lipoma and the underlying cortex of the temporal lobe: pathological features associated with the malformation

Received: 18 June 2004 / Revised: 21 October 2004 / Accepted: 27 October 2004 / Published online: 28 December 2004

Abstract Intracranial lipomas are believed to be congenital malformations rather than true neoplasms, resulting from the abnormal differentiation of the meninx primitiva, the undifferentiated mesenchyme. We report here the surgical pathological features of a lipoma that was located on the cerebral surface of an abnormally formed fissure, and the underlying cortex of the middle temporal gyrus of a 20-year-old woman. The mass was composed of typical adipose tissue in which a large number of blood vessels were present. Thick connective tissue associated with the arachnoid membrane covered the cortical surface. The cortex exhibited a polymicrogyric configuration in which the cortical ribbon was abnormally undulated and excessively folded. Reelin-immunolabeled Cajal-Retzius-cell-like cells were observed frequently in the fused molecular layer. The cortical lamination underlying the molecular layer was poorly defined. Along the border between the connective tissue and cortical surface, there was a narrow zone in which the mesenchymal and neuronal tissues were intermingled, and where immunohistochemical and ultrastructural investigations disclosed disruption of the basal lamina, prominent astrocytosis, and abundant axonal and synaptic profiles. These findings suggest that focal disturbances in cerebral cortical development occur in association with the development of lipomas.

Keywords Lipoma · Polymicrogyria · Cortical dysplasia · Developmental anomaly

A. Kakita (✉)
Department of Pathological Neuroscience,
Resource Branch for Brain Disease Research CBBR,
Brain Research Institute, University of Niigata,
1 Asahimachi, 951-8585 Niigata, Japan
E-mail: kakita@bri.niigata-u.ac.jp
Tel.: +81-25-2270673
Fax: +81-25-2270817

C. Inenaga · H. Takahashi
Department of Pathology, Brain Research Institute,
University of Niigata, 1 Asahimachi,
951-8585 Niigata, Japan

S. Kameyama · H. Masuda · T. Ueno · J. Honma
Department of Neurosurgery and Epilepsy Center,
Nishi-Niigata Chuo National Hospital, 1 Masago,
950-2085 Niigata, Japan

M. Shimohata
Department of Neurology,
Nishi-Niigata Chuo National Hospital, 1 Masago,
950–2085 Niigata, Japan

Introduction

Intracranial lipomas are rare, accounting for about 0.34% of all intracranial tumors [23]. Once thought to be neoplasms of mesodermal origin, intracranial lipomas are now believed to be a type of congenital malformation that results from abnormal persistence and maldifferentiation of the meninx primitiva, the mesenchymal precursor of the leptomeninges, during the development of the subarachnoid cisterns [2, 36].

Lipomas occur preferentially in the midline, and most commonly above the corpus callosum: these are known as interhemispheric lipomas [5, 15, 26, 36]. A large majority of cases of interhemispheric lipoma accompany hypogenesis or agenesis of the corpus callosum [2, 5]. Lipomas can also be detected within the subarachnoid cisterns and spaces, including the cisterna ambiens, chiasmatic and interpeduncular cisterns, cerebellopontine angle, and Sylvian cistern [15, 28, 36]. Examples of lipomas in the Sylvian/insular region, and in particular those located away from the midline [4, 7, 8, 10, 12, 16, 18, 19, 24, 27, 32, 33, 36, 38], are extremely rare, representing approximately 3% [27] or 5% [36] of all intracranial lipomas. Furthermore, there are few reported cases of cerebral surface lipomas [1, 3, 6, 11, 13, 17, 22, 34, 35, 37].

Recently, we had the opportunity of examining a surgical case of lipoma that, unusually, was located on the surface of the temporal lobe distant from the Sylvian fissure. Here we describe the neuropathological features of the mass and the underlying cortex, which indicate that in this case the malformative processes underlying the formation of the lipoma involved the cerebral cortex.

Patient and methods

Patient

A 20-year-old woman visited Nishi-Niigata Chuo National Hospital with a bitemporal headache. A noncontrast-enhanced brain computed tomography (CT) scan disclosed a markedly low-density mass, similar to adipose tissue, with nodular calcification, on the lateral side of the right temporal lobe (Fig. 1A). The mass exhibited a high intensity on magnetic resonance imaging (MRI; Fig. 1B, C), and slight gadolinium enhancement at the edges. No mass effect or surrounding edema was evident. The patient had no family history of neurological diseases or episodes of epileptic seizures. Physical and neurological examinations yielded normal results.

Following a tentative diagnosis of pleomorphic xanthoastrocytoma, en bloc removal of the mass and the surrounding brain tissue was performed. During surgery, an unusually formed sulcus was seen on the surface of the right middle temporal gyrus, where soft, pearly tissue and abnormally accumulated blood vessels were evident (Fig. 2). After surgery, the patient exhibited no neurological deficits or symptoms.

Pathological examination

The surgical specimen was cut in the rostro-caudal axis, and the sections were fixed with phosphate-buffered 20% formalin and embedded in paraffin wax. Serial, 4-μm-thick sections were cut and stained with hematoxylin and eosin, Klüver-Barrera (K-B) stain, the elastica-Goldner method, or Kossa's method for calcium.

Immunohistochemical studies were performed on the formalin-fixed, paraffin-embedded sections using the avidin-biotin-peroxidase complex (ABC) method with a Vectastain ABC kit (Vector, Burlingame, CA). The following primary antibodies were used: rabbit polyclonal antibodies against glial fibrillary acidic protein (GFAP; Dakopatts, Glostrup, Denmark; diluted 1:1,000), laminin (Dako; 1:1,600), and calretinin (Chemicon, Temecula, CA), and monoclonal antibodies against the phosphorylated epitope of neurofilament (SMI-31; Sternberger Monoclonal, Lutherville, MD; 1:1,000), reelin (Chemicon; 1:500), synaptophysin (a gift from Dr. K. Obata; 1:1,000), parvalbumin (Sigma, Saint Louis, MO; 1:500), and Ki-67 antigen (MIB-1, Immunotech, Marseilles, France; 1:100). The chromogen

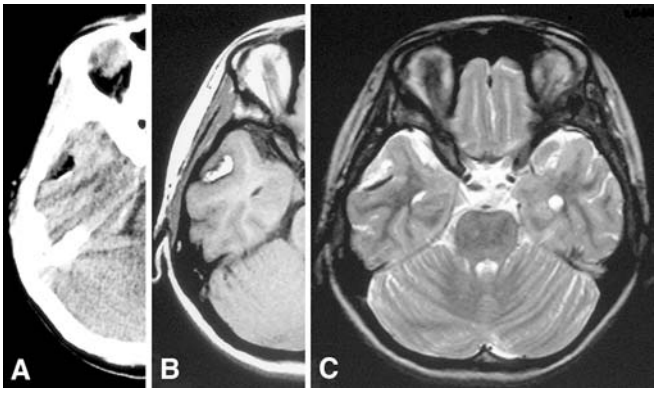

Fig. 1 Preoperative neuroimaging of the lesion. **A** An image from a noncontrast CT scan through the right half of the head shows a low-density mass at the anterolateral portion of the temporal lobe of the cerebrum. The signal is consistent with that of lipid. **B, C** The lesion exhibits a markedly high signal intensity on axial T1-weighted (**B**) and T2-weighted (**C**) magnetic resonance images. A low signal intensity can be seen at the dorsal part of the mass, which corresponds to the high-density area on the CT scan (**A**). This indicates the presence of calcification. Note that no surrounding edema or mass effect is present (*CT* computed tomography)

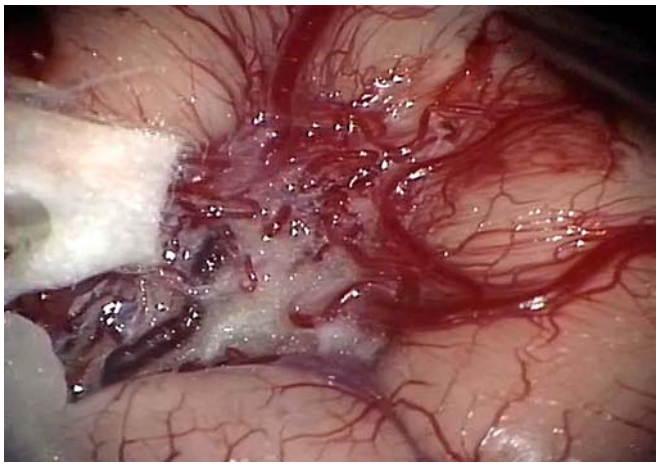

Fig. 2 An intraoperative view showing a soft, pearly-colored mass located in an abnormally formed sulcus of the right middle temporal gyrus. Note that a large number of blood vessels can be seen within the mass and on the cortical surface of the surrounding gyri

►

Fig. 3 A–M Histopathological findings of the lipoma and underlying cortex. **A** A section through the mass and underlying cortex and subcortical white matter. Note the abrupt transition from the normal-looking layered cortex (on *both sides*) to the polymicrogyric cortical ribbon. **B** Higher magnification of the area indicated by *square 1* in **A**, showing the mass, which is typically composed of adipose tissue, thick connective tissue covering the cortical surface, and calcium deposition in the molecular layer of the cortex. **C** Higher magnification of the area indicated by *square 2* in **A** demonstrates that the cortical lamination underlying the undulating molecular layer is poorly defined. **D** Some cells within the molecular layer are labeled by the anti-reelin antibody. **E–G** Higher magnification of the same area as indicated by *square 3* in **A** rotated by 90°. **E** At the border between the connective tissue (*c*) and cortical surface (*n*), a narrow zone is observed in which the mesenchymal and neuronal tissues are intermingled (*cn*). **F** Laminin immunohistochemistry demonstrates that the basal lamina of the pia mater (*arrows*) is disrupted at the "*cn*" zone (*cn* in **E**). **G** GFAP immunohistochemistry discloses prominent astrocytosis at the "*cn*" zone. **H, I** Higher magnification of the same area as indicated by the *square* in **G**. Immunohistochemistry using SMI-31 (**H**) and anti-synaptophysin antibodies (**I**) demonstrates abundant axonal and synaptic profiles, respectively, at the "*cn*" zone. **J, K** Ectopic neurons within the "*cn*" zone. **L, M** Cells within the "*cn*" zone labeled with anti-calretinin (**L**) or anti-parvalbumin (**M**) antibodies. **A, C** Klüver-Barrera stain; **B, E, J, K** hematoxylin and eosin stain; **D, F–I, L, M** immunostained and then counterstained with hematoxylin. *Bar* (in **M**) represents **A** 1.4 mm; **B** 250 μm; **C** 175 μm; **D** 25 μm; **E–G** 340 μm, **H, I** 140 μm; **J, K** 20 μm; **L, M** 10 μm

reaction was developed with 0.02% diaminobenzidine and 0.05% H_2O_2 in 0.05 M TRIS-HCl buffer, pH 7.6, for 10 min.

A few slices were fixed with 3% glutaraldehyde plus 1% paraformaldehyde in 0.1 M phosphate buffer and then processed for electron microscopy. Tissue fragments of a part of the mass and the underlying cortex were post-fixed with 1% osmium tetroxide, dehydrated through a graded ethanol series, and then embedded in Epon 812 resin. Ultrathin sections were cut and stained with uranyl acetate and lead citrate, and examined with a Hitachi H7100 electron microscope at 75 kV.

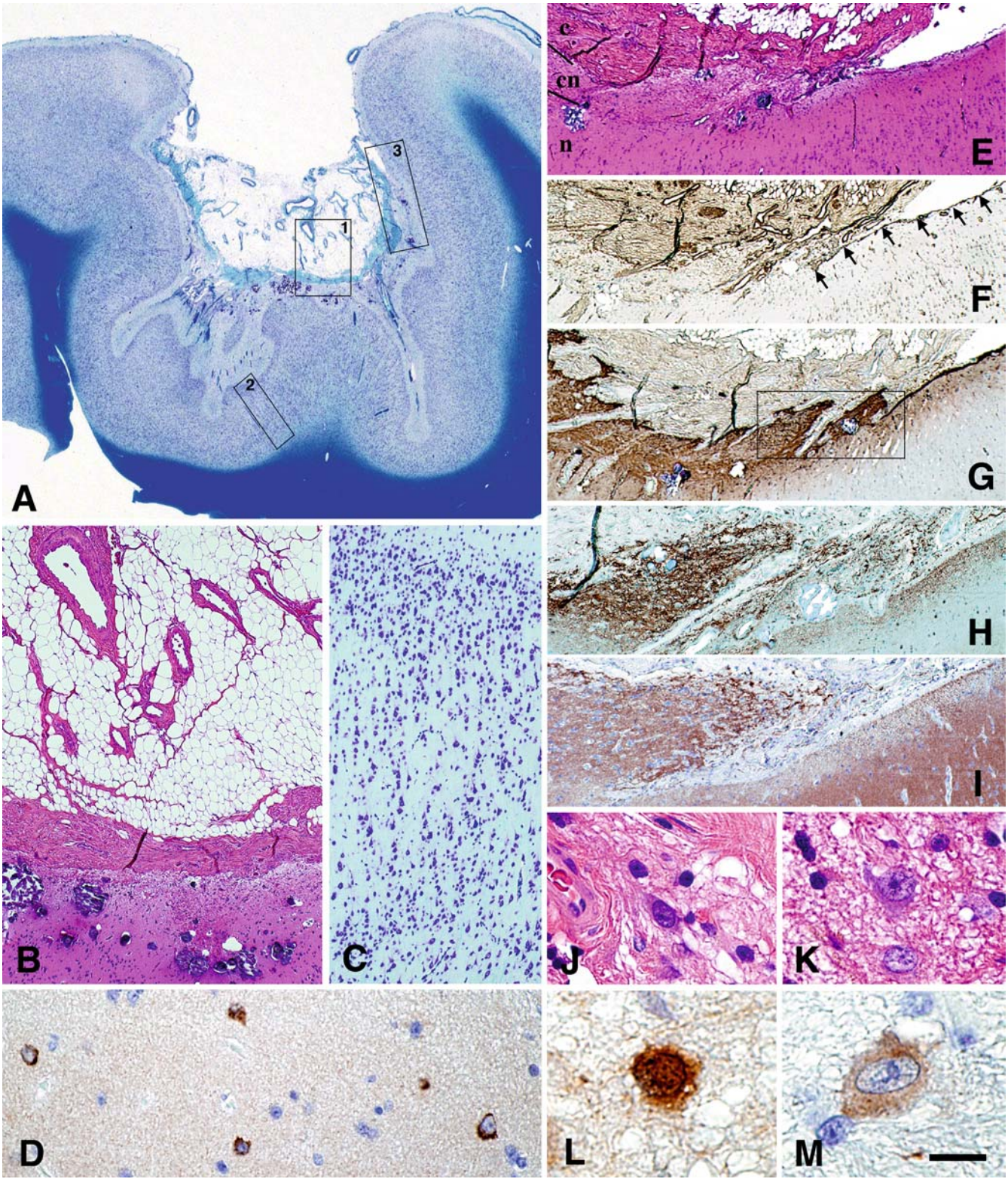

Results

The mass was composed of typical adipose tissue (Fig. 3A, B), leading to a diagnosis of lipoma. MIB-1 immunohistochemistry disclosed no positive cells in the mass. A large number of blood vessels were visible within the mass, but their structure appeared to be normal. There were no leptomeninges covering the convexity of the mass.

Beneath the adipose mass, a thick layer of connective tissue that was associated with the arachnoid membrane covered the cortical surface. The underlying cortex exhibited a polymicrogyric configuration whereby the cortical ribbon was abnormally undulated and excessively folded: the molecular layers of the adjacent gyri appeared to be fused (Fig. 3A). Several vessels impinged vertically in association with the fusion of the mini-convolutions. Conspicuous calcium deposition was seen in the molecular layer (Fig. 3B). The cortical lamination underlying the molecular layer was poorly defined (Fig. 3C). Reelin immunohistochemistry disclosed several labeled cells in the molecular layer (Fig. 3D). In the dysplastic cortex, we detected no MIB-1-immunolabeled cells or cytologically abnormal cells (e.g., giant or dysmorphic neurons and balloon cells), the latter of which are sometimes observed in surgical specimens taken from patients with intractable epilepsy [31].

Along the border between the connective tissue and cortical surface, there was a narrow zone where the mesenchymal and neuronal tissues were intermingled (Fig. 3E), and where the laminin-immunolabeled basal lamina of the pia mater was disrupted (Fig. 3F). At this zone, prominent reactive astrocytosis was observed, as demonstrated by GFAP immunohistochemistry (Fig. 3G). Furthermore, abnormally abundant axonal (Fig. 3H) and synaptic (Fig. 3I) profiles were observed, which were labeled with SMI-31 and synaptophysin antibodies, respectively. There were some well-differentiated neurons within the zone (Fig. 3J, K), and a small proportion of these were labeled by calretinin (Fig. 3L) or parvalbumin (Fig. 3M) antibodies. An ultrastructural investigation of this zone disclosed the occurrence of intermingling of collagen fibrils, dendrites, myelinated fibers, axon terminals, and astrocytic processes (Fig. 4A). A continuous basement membrane separated collagen fibrils from adjacent neurites (Fig. 4B). A large number of synapses were also seen, and dilatation of the postsynaptic structures was frequently observed (Fig. 4C).

Discussion

The first descriptions of intracranial lipomas were achieved mainly through incidental findings at autopsy, and of these only rare examples were located in the Sylvian fissure [4, 7, 24, 38] or on the surface of the cerebral convexity [6, 35]. Subsequently, with the aid of CT and MRI, cases of Sylvian lipoma [1, 8, 10, 12, 16, 18, 19, 28, 32, 33, 36] or lipoma on the cerebral surface [1, 3, 11, 13, 17, 22, 34, 37] have been identified. Bakshi et al. [1] studied a large consecutive series of intracranial lipomas neuroradiologically with the aid of a variety of conventional and advanced MRI techniques, methods that have yielded fairly reliable in vivo diagnoses of lipoma. Their series also suggested the possibility that cerebral lipomas might occur in lateral locations more frequently than had been reported previously [1]. On the other hand, reports of cases in which surgery was performed and hence histological confirmation of lipoma was possible are limited [3, 8, 10, 12, 13, 16, 18, 28, 34, 37]. In the present case, en bloc removal of the cerebral surface lipoma and surrounding brain tissue was performed, and this enabled us to examine in detail the histopathological features of the mass as well as the underlying cerebral cortex.

In this case, hypervascularization was observed adjacent to and within the lipoma (Fig. 2). A variety of vascular abnormalities including hypervascularization [3, 8, 22], venous angioma [16], dilatation and tortuosity of the feeding arteries [34], abnormal arterial branches [32], and saccular aneurysm [12] have been described in cases with cerebral lipoma. Thus, development of a lipoma may also involve vascular abnormalities.

In the present case, the lipoma was located on the surface of the abnormally formed sulcus of the temporal lobe (Fig. 2), and polymicrogyria of the cortex underlying the mass was observed (Fig. 3A). There are reports of cortical abnormalities associated with cerebral lipoma. For example, two autopsy cases have been described in which large masses were accompanied by polymicrogyria [7, 35]. In addition, dysplastic features have been identified by MRI, including pachygyria-like abnormalities and subcortical nodular heterotopia in a case of Sylvian lipoma [16], and an abnormal sulcal pattern and thickened cortical ribbon adjacent to lipomas on the surface of the parietal [32] and frontal [34] lobes. Britt et al. [3] reported a surgical case of frontoparietal lipoma in which marked architectural disorganization and focal penetration of the fibroadipose lesion into the brain parenchyma were noted: such features are consistent with those observed in the case described here. Thus, the formation of a cerebral lipoma might be a part of complex malformation that also involves sulcus formation and cortical development within its vicinity.

Several reelin-immunolabeled cells were observed in the molecular layer of the polymicrogyric cortex (Fig. 3D). The cells could be regarded as Cajal-Retzius cells [28]. Eriksson et al. [9] examined a variety of polymicrogyric conditions in cases ranging in age from 21 gestational weeks to 10 years, and identified persistent reelin-expressing Cajal-Retzius cells in the molecular layer, consistent with the present case. The significance and functions of these persistent cells in this adult patient remain unclear. However, it is known that an early and fundamental step of cortical laminar organization is critically controlled by the activities of

reelin-positive cells in the molecular layer [14], and abnormal reelin activity in development is associated with abnormal cortical folding [9]. Therefore, it seems likely that disruption of the expression of reelin and its downstream signaling pathway may have resulted in the ill-defined cortical lamination observed in this case.

Intermingling of mesenchymal and neuronal tissue was evident at the border between the connective tissue and the cortical surface (Fig. 3E), where abnormally abundant axonal (Figs. 3H, 4A) and synaptic (Figs. 3I, 4C) profiles, and astrocytic processes (Figs. 3G, 4A) were also observed. These features indicate that abnormal sprouting and synaptic connections, in conjunction with active astrocytic reactions, had been occurring in this unusual cortical environment. In addition, we observed mature neurons in that area (Fig. 3J, K). To assess the cell-fate characteristics of the neurons that were extruded into the heterotopic foci, we applied immunohistochemistry and found that a proportion of these neurons were labeled with antibodies against the calcium-binding proteins calretinin and parvalbumin (Fig. 3L, M). It has been shown that calcium-binding proteins are contained in GABAergic interneurons, and that during normal development they settle in particular layers of the neocortex [29]. It is plausible that some over-migrated progenitor cells survived and differentiated into mature forms even within such unusual surroundings, rather than undergoing apoptotic cell death.

We observed basement membrane separating the collagen and neurites (Fig. 4B). With respect to the heterotopic location of the neuronal cell elements, it appears possible that in situ, the proliferated mesenchymal fibers may play an important role in the for-

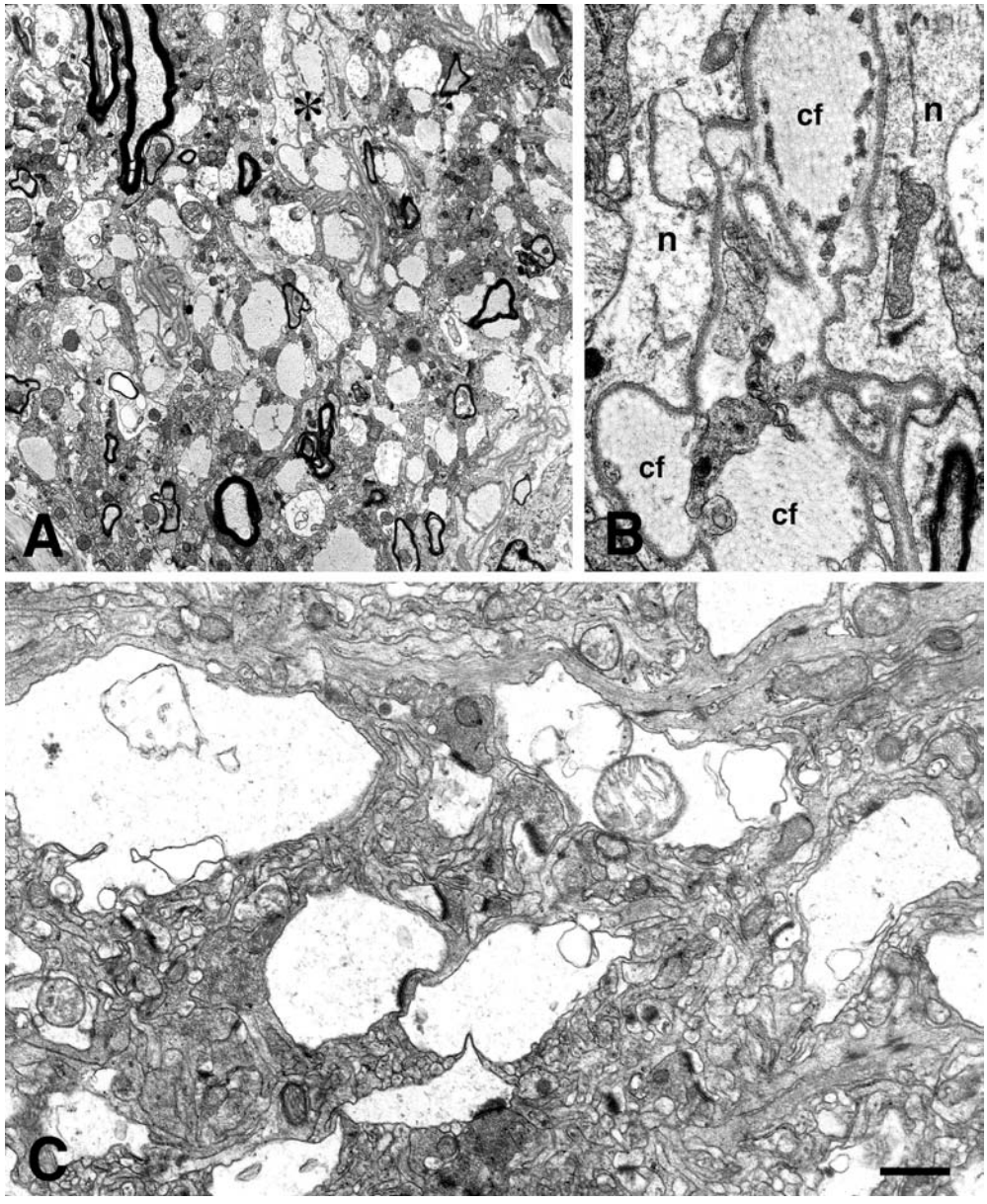

Fig. 4 A–C Electron micrographs of the cortical surface underlying the lipoma. **A** An area showing conspicuous intermingling of collagen fibrils, neuronal dendrites, myelinated fibers, axon terminals, and astrocytic processes. **B** Higher magnification of the area indicated by the *asterisk* in **A**, showing a continuous basement membrane separating the collagen fibrils (*cf*) from the adjacent neurites (*n*). **C** Many synapses with frequent dilatation of the postsynaptic structures are seen. *Bar* (in **C**) represents **A** 2.5 μm; **B** 630 nm; **C** 900 nm

mation of these structures. This reaction seems to be common in both humans and other animals. Indeed, we have previously observed similar, but more premature structures in autopsied human brains: in an incidentally identified leptomeningeal glioneuronal heterotopia (LGH) of an infant, and the tumor tissue of primary leptomeningeal glioma [20], as well as in experimentally induced LGH in rats [21].

The patient described here complained of a headache; however, it is highly likely that this association was coincidental rather than causative. On the other hand, epileptic seizures have been noted in a large proportion of patients with Sylvian lipoma [7, 8, 10, 16, 18, 27, 32, 33] and cerebral surface lipoma [3, 11, 13, 17, 37]. Although this patient has never experienced seizures, the possibility that she will suffer from them in the future cannot be excluded since the postsynaptic alterations observed (Fig. 4C) may be an early change associated with local excessive discharges or minibursts. Similar ultrastructural alterations have been observed in the hippocampus of kainate-treated rats [30], experimental spongiform encephalopathy in chimpanzees [25], and surgical specimens taken from patients with intractable epilepsy (unpublished observation).

When encountering a mass on the cerebral surface, lipoma should be considered as a possible etiology, especially in patients with epilepsy, although it should also be recognized that such cases are very rare. The present case provides information about the histogenesis of the malformed cortex underlying the lipoma mass, which might be useful for future diagnoses.

Acknowledgments The authors thank C. Tanda, S. Egawa, Y. Ohta, J. Takasaki, and N. Kaneko for technical assistance, and M. Machida for secretarial assistance. This work was supported in part by a Grant-in Aid for Scientific Research (no. 16500214) from the Ministry of Education, Culture, Sports, Science, and Technology, Japan (A.K.).

References

1. Bakshi R, Shaikh ZA, Kamran S, Kinkel PR (1999) MRI findings in 32 consecutive lipomas using conventional and advanced sequences. J Neuroimaging 9:134–140
2. Barkovich AJ (1995) Congenital malformations of the brain and skull. In: Pediatric neuroimaging, 2nd edn. Raven Press, New York, pp 177–275
3. Britt PM, Bindal AK, Balko MG, Yeh HA (1993) Lipoma of the cerebral cortex: case report. Acta Neurochir (Wien) 121:88–92
4. Cserni G (1993) Intracranial lipoma of the Sylvian region. Neuropathol Appl Neurobiol 19:282–285
5. Demaerel P, Van de Gaer P, Wilms G, Baert AL (1996) Interhemispheric lipoma with variable callosal dysgenesis: relationship between embryology, morphology, and symptomatology. Eur Radiol 6:904–909
6. Demus H (1967) Neue Gesichtspunke zur Entstehung der pialen Lipome. Arch Psychiatr Nervenkr 209:426–442
7. Dragojevíc S, Mehraein P, Bock HJ (1973) Beobachtung eines Lipoms der Temporalregion mit rindenmissbildung und Epilepsie. Klinisch-pathologische Studie (in German with English abstract). Arch Psychiatr Nervenkr 217:335–342
8. Dyck P (1985) Sylvian lipoma causing auditory hallucination: case report. Neurosurgery 16:64–67
9. Eriksson SH, Thom M, Heffernan J, Lin WR, Harding BN, Squier MV, Sisodiya SM (2001) Persistent reelin-expressing Cajal-Retzius cells in polymicrogyria. Brain 124:1350–1361
10. Feldman RP, Marcovici A, LaSala PA (2001) Intracranial lipoma of the sylvian fissure. Case report and review of the literature. J Neurosurg 94:515–519
11. Fujii Y, Konishi Y, Kriyama M, Hori C, Sudo M (1993) Lipoma on surface of centroparietal lobes. Pediatr Neurol 9:144–146
12. Futami K, Kimura A, Yamashita J (1992) Intracranial lipoma associated with cerebral saccular aneurysm. J Neurosurg 77:640–642
13. Gabrovski S, Poptodorov G, Aleksiev A, Krustev E, Dimitrov D (1999) [Lipoma of the temporal lobe] (in Bulgarian with English abstract). Khirurgiia (Sofiia) 55:55–59
14. Gleeson JG, Walsh CA (2000) Neuronal migration disorders: from genetic diseases to developmental mechanisms. Trends Neurosci 23:352–359
15. Gómez-Gosálvez FA, Menor-Serrano F, Téllez de Meneses-Lorenzo M, Aleu Pérez-Gramunt, Sala-Sánchez AG, Rubio-Soriano A, Carbonell-Nadal J, Mulas F (2003) [Intracranial lipomas in pediatrics: a retrospective study of 20 patients] (in Spanish with English abstract). Rev Neurol 37:515–521
16. Guye M, Gastaut JL, Bartolomei F (1999) Epilepsy and perisylvian lipoma/cortical dysplasia complex. Epileptic Disord 1:69–73
17. Hädecke J, Buchfelder M, Triebel H-J, Schneyer U (1997) Multiple intracranial lipoma: a case report. Neurosurg Rev 20:282–287
18. Hatashita S, Sakakibara T, Ishii S (1983) Lipoma of the insula. Case report. J Neurosurg 58:300–302
19. Hayashi T, Shojima K, Yamamoto M, Hashimoto T, Fukuzumi A, Honda E (1983) [Intracranial lipomas. A report of six cases] (in Japanese with English abstract). No to Shinkei 35:257–268
20. Kakita A, Wakabayashi K, Takahashi H, Ohama E, Ikuta F, Tokiguchi S (1992) Primary leptomeningeal glioma: ultrastructural and laminin immunohistochemical studies. Acta Neuropathol 83:538–542
21. Kakita A, Wakabayashi K, Su M, Piao Y-S, Takahashi H (2001) Experimentally induced leptomeningeal glioneuronal heterotopia and underlying cortical dysplasia of the lateral limbic area in rats treated transplacentally with methylmercury. J Neuropathol Exp Neurol 60:768–777
22. Kannuki S, Okajima K, Sato K, Kusaka K, Matsumoto K (1986) [Intracranial lipoma of the temporal lobe. Report of a case and review of the literature] (in Japanese with English abstract). No Shinkei Geka 14:379–384
23. Kazner E, Stochdorph O, Wende S, Grumme T (1980) Intracranial lipoma. Diagnostic and therapeutic considerations. J Neurosurg 52:234–245
24. Krainer L (1935) Die Hirn- und Rückenmarkslipome. Virchows Arch Pathol Anat 295:107–142
25. Lampert PW, Gajdusek DC, Gibbs CJ Jr (1971) Experimental spongiform encephalopathy (Creutzfeldt-Jacob disease) in chimpanzees. Electron microscopic studies. J Neuropathol Exp Neurol 30:20–32
26. Maiuri F, Cirillo S, Simonetti L, De Simone MR, Gangemi M (1988) Intracranial lipomas. Diagnostic and therapeutic considerations. J Neurosurg Sci 32:161–167
27. Maiuri F, Cirillo S, Simonetti L (1989) Lipoma of the sylvian region. Clin Neurol Neurosurg 91:321–323
28. Meyer G, Goffinet AM, Fairén A (1999) What is a Cajal-Retzius cell? A reassessment of a classical cell type based on recent observations in the developing neocortex. Cereb Cortex 9:765–775
29. Nieuwenhuys R (1994) The neocortex. An overview of its evolutionary development, structural organization and synaptology. Anat Embryol (Berl) 190:307–337

30. Olney JW, Fuller T, de Gubareff T (1979) Acute dendrotoxic changes in the hippocampus of kainite treated rats. Brain Res 176:91–100
31. Palmini A, Najm I, Avanzini G, Babb T, Guerrini R, Foldvary-Schaefer N, Jackson G, Lüders HO, Prayson R, Spreafico R, Vinters HV (2004) Terminology and classification of the cortical dysplasias. Neurology 62 (Suppl 3):S2–S8
32. Saatci I, Askan C, Renda Y, Besim A (2000) Parietal lipoma associated with cortical dysplasia and abnormal vasculature: case report and review of the literature. AJNR Am J Neuroradiol 21:1718–1721
33. Sarioglu AC, Kaynar MY, Hanci M, Uzan M (1999) Sylvian fissure lipomas: case reports and review of the literature. Br J Neurosurg 13:386–388
34. Sasaki H, Yoshida K, Wakamoto H, Otani M, Toya S (1996) Lipomas of the frontal lobe. Clin Neurol Neurosurg 98:27–31
35. Scherer E (1936) Über die pialen Lipome des Gehirns. Beitrag eines Falles von ausgedehnter meningealer Lipomatose einer Grossirnhemisphäre bei Mikrogyrie. Z Neurol 154:45–61
36. Truwit CL, Barkovich AJ (1990) Pathogenesis of intracranial lipoma: an MR study in 42 patients. AJR Am J Roentgenol 155:855–864
37. Vela-Yebra R, Pastor-Pons E, Garcia Del Moral-Garrido R, Hervas-Navidad R, Sanchez-Alvarez JC (2002) [Lipoma of the cerebral convexity and refractory focal epilepsy] (in Spanish with English abstract). Rev Neurol 34:742–745
38. Yalcin S, Fragoyannis S (1966) Intracranial lipoma. Case report. J Neurosurg 24:895–897